Inorganic Chemistry

Article

pubs.acs.org/IC

Charge and Spin-State Characterization of Cobalt Bis(*o*-dioxolene) Valence Tautomers Using Co K*β* X-ray Emission and L-Edge X-ray Absorption Spectroscopies

H. Winnie Liang,[*,†,‡] Thomas Kroll,[§] Dennis Nordlund,[§] Tsu-Chien Weng,[∥] Dimosthenis Sokaras,[§] Cortlandt G. Pierpont,[#] and Kelly J. Gaffney[*,‡,§]

[†]Department of Chemistry, Stanford University, Stanford, California 94305, United States

[‡]PULSE Institute, SLAC National Accelerator Laboratory, Menlo Park, California 94025, United States

[§]Stanford Synchrotron Radiation Lightsource (SSRL), SLAC National Accelerator Laboratory, Menlo Park, California 94025, United States

[∥]Center for High Pressure Science & Technology Advanced Research, Pudong, Shanghai 201203, P. R. China

[#]Department of Chemistry and Biochemistry, University of Colorado, Boulder, Colorado 80309, United States

Supporting Information

ABSTRACT: The valence tautomeric states of Co(phen)-(3,5-DBQ)$_2$ and Co(tmeda)(3,5-DBQ)$_2$, where 3,5-DBQ is either the semiquinone (SQ$^-$) or catecholate (Cat^{2-}) form of 3,5-di-*tert*-butyl-1,2-benzoquinone, have been examined by a series of cobalt-specific X-ray spectroscopies. In this work, we have utilized the sensitivity of 1s3p X-ray emission spectroscopy (K*β* XES) to the oxidation and spin states of 3d transition-metal ions to determine the cobalt-specific electronic structure of valence tautomers. A comparison of their K*β* XES spectra with the spectra of cobalt coordination complexes with known oxidation and spin states demonstrates that the low-temperature valence tautomer can be described as a low-spin Co^{III} configuration and the high-temperature valence tautomer as a high-spin Co^{II} configuration. This conclusion is further supported by Co L-edge X-ray absorption spectroscopy (L-edge XAS) of the high-temperature valence tautomers and ligand-field atomic-multiplet calculations of the K*β* XES and L-edge XAS spectra. The nature and strength of the magnetic exchange interaction between the cobalt center and SQ$^-$ in cobalt valence tautomers is discussed in view of the effective spin at the Co site from K*β* XES and the molecular spin moment from magnetic susceptibility measurements.

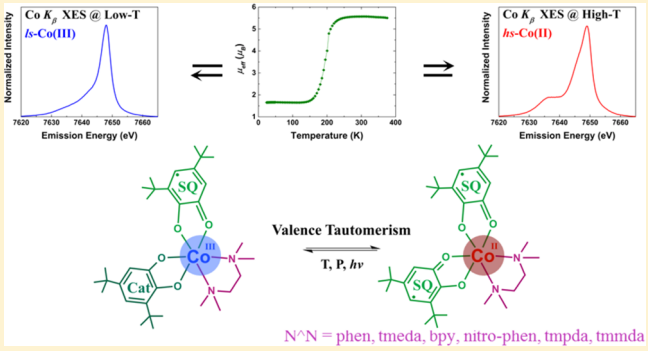

INTRODUCTION

The ability to generate long-lived metastable electronic states with external stimuli makes the phenomena of spin crossover (SCO) and valence tautomerism (VT) in 3d transition-metal complexes a subject of great interest, with potential applications in spintronic devices, data storage, and molecular switches.[1−6] The thermodynamic ease with which coordination complexes with redox-active ligands can convert between distinct charge and spin states has also been associated with catalytic activity in organic transformations.[7−9] VT corresponds to an intramolecular electron transfer between a redox-active metal center and a redox-active ligand coupled to a change in spin multiplicity, or a spin crossover, at the metal center.[10−16] Furthermore, as is true for SCO transitions, VT transitions are typically accompanied by distinct and reversible changes in the structural, optical, and magnetic properties of the metal complexes.[15,17−19] They have been observed in transition-metal complexes of Mn, Fe, Co, Ni, Cu, Rh, Ru, and Ir with a variety of redox-active ligand types, including *o*-dioxolenes, porphyrins, phenoxyl ligands, ferrocenes, and tetrathiafulvalene.[12,20−27] In general, metal complexes displaying VT transitions meet the following two electronic requirements: (1) the degree of covalency in the interaction between a metal ion and a redox-active ligand must be small, and (2) their frontier orbitals must be of similar energy.[2,12]

Cobalt bis(*o*-dioxolene) coordination compounds represent an archetypical series of valence tautomeric complexes, where the term "*o*-dioxolene" denotes the redox series of neutral *o*-benzoquinone (*o*-BQ), monoanionic semiquinone (SQ$^-$), and catecholate dianion (Cat^{2-}), without specifying the substituents on the benzene ring. In [Co^{III}(3,5-DBSQ)(3,5-DBCat)(N^N)], where 3,5-DBSQ/3,5-DBCat is a 3,5-di-*tert*-butyl-substituted semiquinone/catecholate and N^N is a bidentate N-donor

Received: July 19, 2016

DOI: 10.1021/acs.inorgchem.6b01666
Inorg. Chem. XXXX, XXX, XXX−XXX

Scheme 1. Illustration of VT in Co(tmeda)(3,5-DBQ)$_2$ with the Co 3d and Ligand π^* Orbitals Shown, Where DBQ Can Either Be a Singly-Reduced Semiquinone (SQ^-) or a Doubly-Reduced Catecholate Ligand (Cat^{2-}) Depending on the Valence Tautomeric State of the Complex at the Specified Temperature, with the Co^{III}(tmeda)(3,5-DBSQ)(3,5-DBCat) Form Favored at Low Temperature and the Co^{II}(tmeda)(3,5-DBSQ)$_2$ Form Favored at High Temperature[a]

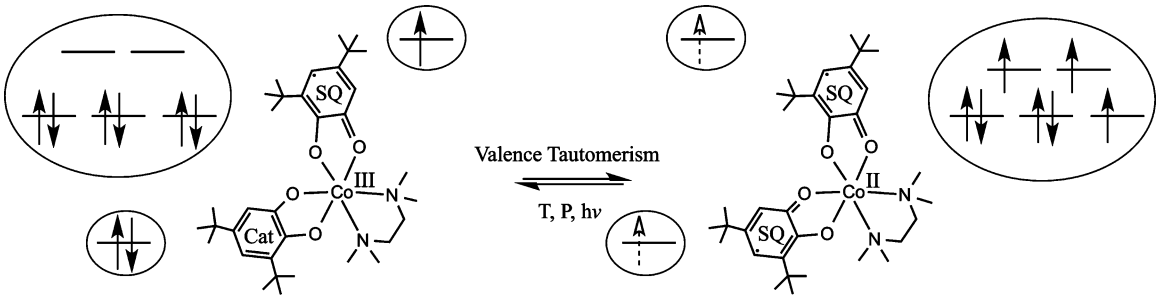

[a]The redox series of *o*-BQ can be described as $Cat^{2-} \rightarrow SQ^- + e^- \rightarrow$ *o*-BQ + $2e^-$. Note that the coordination geometry at the Co center is assumed to be pseudooctahedral, with the metal d level split into the t_{2g} and e_g sets, whereas the dashed electron arrows on SQ^- are a reminder of the weak coupling interactions between unpaired electrons on the ligands and those at the metal center.

coligand such as 1,10-phenanthroline (phen) and *N,N,N′,N′*-tetramethylethylenediamine (tmeda), intervalence electron transfer nominally involves the transfer of an electron from the Cat^{2-} π^* orbital to the low-spin (ls)-Co^{III} center to form a SQ^- and a high-spin (hs) Co^{II} (Scheme 1). It has been shown that valence tautomeric interconversion can be driven by changes in the temperature (T) and pressure (P), as well as by irradiation with lasers or soft X-rays.[28−37] In this work, all cobalt valence tautomers will be referred to as either Co(N^N) or Co(N^N)(3,5-DBQ)$_2$, where N^N specifies the coligand identity; DBQ can refer to either semiquinone or catecholate, depending on the valence tautomeric state of the complex at the specified temperature.

Our study addresses the number of electronic configurations needed to accurately describe the electronic structure of the low- and high-T valence tautomeric states, an open question despite extensive studies of cobalt bis(*o*-dioxolene) valence tautomers. In 2002, LaBute et al.[38,39] used a variational configuration interaction approach and Co K-edge X-ray absorption spectroscopy (K-edge XAS) to investigate the Co(phen) system. They concluded that multiple configurations must be included in the calculations to accurately reproduce the energy difference between the low- and high-T states and the 1s3d preedge absorption features in K-edge XAS, with the high-T valence tautomeric phase having both hs-Co^{II} and hs-Co^{III} character and the low-T phase having both ls-Co^{II} and ls-Co^{III} character. An additional theoretical study by Sato et al.[40] also highlights the potential significance and energetic accessibility of a ls-Co^{II} configuration in VT. On the basis of their study of the minimum-energy crossing points and the potential energy paths connecting distinct spin states of cobalt, they proposed a mechanism in which the ls-Co^{II} species can serve as an intermediate state in the thermally driven interconversion of ls Co^{III} to hs Co^{II}.

In this work, we present a Co 1s3p X-ray emission spectroscopy (Kβ XES) and Co L-edge X-ray absorption spectroscopy (L-edge XAS) investigation of the electronic structures of the Co(phen) and Co(tmeda) valence tautomers. Both of these spectroscopies have been well demonstrated to characterize the charge, spin, and metal−ligand covalency of 3d coordination complexes from the metal's perspective, which will be used to investigate the importance of multiconfigurational interactions and the strength of the Co−SQ^- magnetic exchange interaction in valence tautomers. The atomic specificity of X-ray spectroscopies differentiates them from conventional techniques such as electron paramagnetic resonance (EPR), UV−visible, IR, NMR, and magnetic susceptibility. While these non-X-ray-based methods allow the interconversion process to be monitored in a temperature-dependent manner, they lack the capability to discern changes in the spin and charge configurations at the Co center. The strong exchange interaction between the unpaired 3p and 3d electrons in the final state created by X-ray emission controls the relative intensity and energetic positions of the K$\beta_{1,3}$ and Kβ' spectral features in the XES spectrum and makes the measurement sensitive to the effective metal spin and charge states, which can be further modulated by metal−ligand covalency.[41−44] We have also used Co L-edge XAS measurements and ligand-field atomic-multiplet calculations to investigate the cobalt-specific electronic structure at high temperature. These measurements and calculations complement Kβ XES and enable a more comprehensive determination of the importance of a hs-Co^{III} configuration in the high-T valence tautomers. Both XES and XAS measurements, as well as atomic-multiplet calculations, demonstrate that both valence tautomeric states can be robustly described with single-electron configurations for cobalt and provide no evidence for the hs-Co^{III} configuration proposed by previous researchers.[39] During our measurements, we also observed the occurrence of soft X-ray-induced VT in our low-T L-edge XAS data that is consistent with the work of Poneti et al.[32] and the possibility of hard X-ray-induced VT with aromatic nitrogen coligands. Given prior reports of interconversions induced by hard X-rays,[45−50] this, in turn, has limited our XES study of the electronic structure of low-T valence tautomers to the Co(tmeda) complex.

By combining the cobalt-specific charge and spin states derived from Co Kβ XES with the molecular spin moment extracted from magnetic susceptibility measurements, we proceed to address the strength of the magnetic exchange interaction between unpaired spins on the SQ^- ligands and the Co center in high-T valence tautomers. These measurements show a spin moment of $S = {}^3/_2$ for both the Co ion and the entire molecule, an observation consistent with weak magnetic exchange interactions between SQ^- and the hs d^7 metal center.

■ EXPERIMENTAL SECTION

Sample Preparation. ls- and hs-Co^{III} and -Co^{II} model compounds were purchased from Sigma-Aldrich and used as they were received:

DOI: 10.1021/acs.inorgchem.6b01666
Inorg. Chem. XXXX, XXX, XXX−XXX

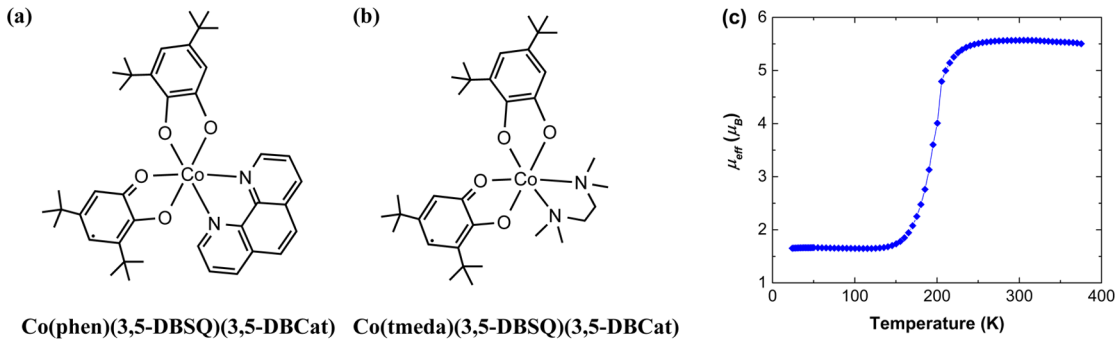

Figure 1. Cobalt-containing valence tautomeric complexes investigated in this work: (a) Co(phen)(3,5-DBQ)$_2$·C$_6$H$_5$CH$_3$ and (b) Co(tmeda)(3,5-DBQ)$_2$·0.5C$_6$H$_6$. (c) Temperature-dependent effective magnetic moment of Co(tmeda)(3,5-DBQ)$_2$·0.5C$_6$H$_6$. Molecular structures are expressed in their low-T valence tautomeric state. Note that Q can be either semiquinone or catecholate, depending on the valence tautomeric state of the complex at the specified temperature.

tris(ethylenediamine)cobalt(III) chloride dihydrate, cobalt(III) acetylacetonate, and cobalt(II) acetylacetonate, namely, [Co(en)$_3$]Cl$_3$·2H$_2$O, Co(acac)$_3$, and Co(acac)$_2$, respectively. Compounds (a) Co(phen)(3,5-DBQ)$_2$·C$_6$H$_5$CH$_3$ and (b) Co(tmeda)(3,5-DBQ)$_2$·0.5C$_6$H$_6$ (see Figure 1), along with Co$_4$(3,5-DBSQ)$_8$ and Co(phen)$_3$·Cl$_2$·4H$_2$O, were synthesized according to literature procedures[51−54] with reagents and solvents purchased directly from Sigma-Aldrich. The final products were characterized in toluene by UV−visible and IR absorption spectroscopies and confirmed with elemental analysis. Samples for X-ray emission experiments were ground into a fine powder, packed tightly into a 1.0-mm-thick aluminum cell, and sealed with 63.5 μm kapton tape. For air-sensitive samples or samples going into a vacuum, as in soft X-ray measurements, the preparation step was done inside a glovebox under an inert N$_2$ atmosphere.

XES Data Collection and Processing. Kβ X-ray emission spectra were collected at SSRL beamline 6-2 with ring conditions of 3.0 GeV and 500 mA. The incident beam energy was set to 8.0 keV using a LN$_2$-cooled Si(111) monochromator that was calibrated with a cobalt foil, providing ~2×10^{13} photons s^{-1} in a 0.15×0.4 mm spot size and an energy resolution ($\Delta E/E$) of 1×10^{-4}. Emitted X-rays were energy-selected using four spherically bent Ge(444) crystals arranged in a Rowland geometry and were detected with a silicon drift detector. The incident flux was measured using a helium-filled ion chamber just upstream of the sample. A helium-filled flight path was used between the sample, crystal analyzers, and detector to minimize signal attenuation. X-ray-induced damage was assessed by collecting successive X-ray scans on a single spot; multiple spots were used when needed for each sample. Temperature control of the samples was achieved using a combination of a helium cryostat and a resistive heater.

In all of the samples, two scans were taken per spot, for a total of six scans per sample. These scans were then each normalized by its incident flux and averaged together to yield the final spectrum in PyMca. Each average spectrum was further scaled by its total intensity under the curve to allow for comparison.

L-Edge XAS Data Collection and Processing. Co L-edge X-ray absorption spectroscopy was performed at SSRL beamline 10-1. The beamline is equipped with a 6 m spherical grating monochromator operated with a 1000 lines mm^{-1} grating (Co 2p XAS) and 20 μm entrance and exit slits, providing 10^{11} photons s^{-1} at a resolution $\Delta E/E$ of 2×10^{-4} in a beam spot of 1.0 mm^2.

All data were acquired in the temperature range of 90−298 K, where the samples were cooled by LN$_2$ and under an ultrahigh vacuum (~10^{-9} Torr). Both the total electron yield (TEY, measured via the sample drain current, SC) and Auger electron yield (AEY, measured with a cylindrical mirror analyzer coupled to a channeltron) were recorded simultaneously. All spectra were normalized by the incoming flux, measured from a thin grid with freshly evaporated gold, positioned upstream of the sample chamber. A reference sample with several transition-metal oxides, intercepting a few percent of the beam upstream and recorded simultaneously, was used to calibrate the energy of the cobalt scans with a relative energy precision of 25 meV. All powder samples were thoroughly mixed with 50% graphite by volume and affixed to an aluminum sample holder using conductive carbon tape. The AEY was used for the XAS spectra in this study. Background correction was performed using the statistics-sensitive nonlinear iterative peak-clipping algorithm in PyMca. Each spectrum was an average of 4−5 scans, with each scan taken at a different spot on the sample tape.

Ligand-Field Atomic-Multiplet Calculations. Atomic-multiplet calculations were performed using the *CTM4XAS 5.5* program.[55,56] The effects of covalent metal−ligand mixing were included as a screening of the 3d−3d Coulomb repulsion, which manifested itself in the reduction of F_{dd}, F_{pd}, and G_{pd} Slater integrals to 75% of their atomic values, while an unscaled value was used for the 2p core state and 3d valence state spin−orbit coupling.

Magnetic Measurements. Magnetic susceptibility measurements were performed using Quantum Design's MPMS3, a SQUID magnetometer, in an applied field of 5000 Oe and with a ramp of 5 K min^{-1} in the temperature range of 25−375 K. The Curie−Weiss law was applied in the data analysis to yield an adjusted χ quantity, which can be related to $\mu_{eff} = \sqrt{8\chi T}$. When valence tautomerization is described as an equilibrium between two redox isomeric states (low-T ⇄ high-T), $\mu_{eff}^2 = f_{ls}\mu_{eff,ls}^2 + f_{hs}\mu_{eff,hs}^2$ and $1 = f_{ls} + f_{hs}$, where $\mu_{eff,ls}$ is the limiting value of the effective magnetic moment for the low-T, low-spin valence tautomeric state and $\mu_{eff,hs}$ is the limiting value of the effective magnetic moment for the high-T, high-spin valence tautomeric state. The mole fraction of the high-T, high-spin valence tautomeric state, f_{hs}, can be determined and plotted as a function of temperature.

■ RESULTS AND DISCUSSION

While different cobalt valence tautomers have been extensively investigated by various methods,[12,57−59] selective observations of the electronic structure at the Co center have yet to be accomplished. In this work, we utilize temperature-dependent magnetic susceptibility of the valence tautomeric complexes Co(phen) and Co(tmeda) as a guide for identifying their redox isomeric states and later as a complementary tool, along with our X-ray spectroscopic measurements, for understanding the Co−SQ$^-$ magnetic exchange interactions at high temperature. To begin, Kβ XES will be used to investigate and assign the oxidation and spin states of the cobalt complexes in their VT states. Followed by a combination of Co L-edge XAS and ligand-field atomic-multiplet calculations, the high-T valence tautomeric state will be studied in more detail to address its electronic configuration. Last, metal−ligand interactions in valence tautomers will be discussed in the context of our element-specific X-ray- and molecular-based measurements.

DOI: 10.1021/acs.inorgchem.6b01666
Inorg. Chem. XXXX, XXX, XXX−XXX

I. Assignment of Oxidation and Spin States of Valence Tautomers at Low Temperature Using Kβ XES. Comparing the Kβ XES spectra of Co(phen)(3,5-DBQ)$_2$ and Co(tmeda)(3,5-DBQ)$_2$ to those of cobalt model compounds with well-established charge and spin states provides a powerful approach to characterizing the electronic structure of the valence tautomers. We use two familiar ls-Co^{III} complexes, [Co(en)$_3$]Cl$_3$·2H$_2$O and Co(acac)$_3$, for comparison because they share a similar ligand environment and coordination geometry with the cobalt valence tautomers under investigation. [Co(en)$_3$]Cl$_3$·2H$_2$O (en = ethylenediamine) is an excellent model complex because of its structural similarity to one of the valence tautomers, Co(tmeda)(3,5-DBQ)$_2$, whereas the acetylacetonate (acac) ligand in Co(acac)$_3$ resembles the "O−C═C−O" moiety in *o*-dioxolene.

The Kβ XES spectra of Co(tmeda) and Co(phen), taken at 36 and 34 K, respectively, are compared with [Co(en)$_3$]Cl$_3$·2H$_2$O and Co(acac)$_3$, as shown in Figures 2 and 3.

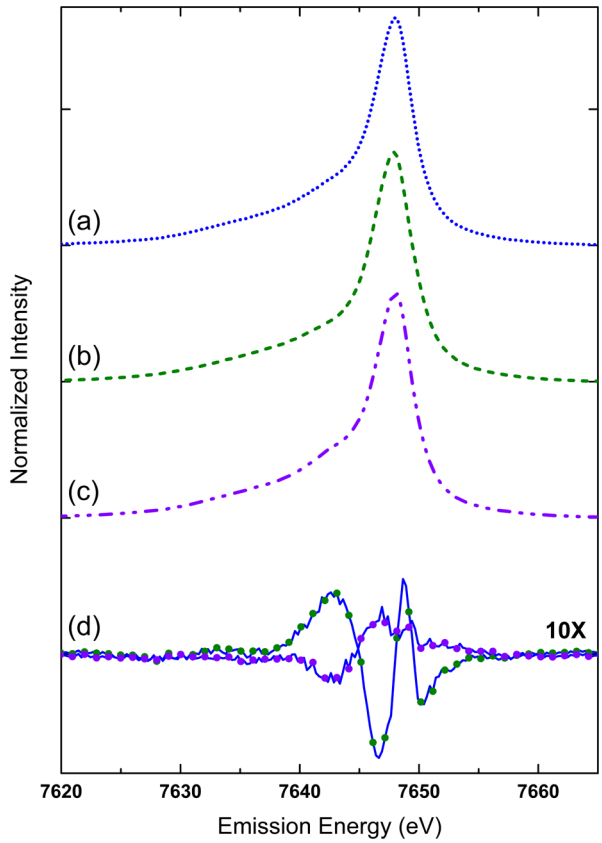

Figure 2. Co Kβ XES of (a) Co(tmeda)(3,5-DBQ)$_2$ taken at 36 K (blue, dotted line), (b) [Co(en)$_3$]Cl$_3$·2H$_2$O (dark green, dashed line), (c) Co(acac)$_3$ (purple, dash-dot-dotted line), where parts b and c are ls-Co^{III} reference model complexes, and (d) the difference spectra, defined as $I - I_{ref}$, of the low-*T* valence tautomer and ls-Co^{III} model complexes: Co(tmeda)(3,5-DBQ)$_2$ at 36 K with [Co(en)$_3$]Cl$_3$·2H$_2$O (blue solid line + dark green solid circle) and Co(acac)$_3$ (blue solid line + purple solid circle).

Co(phen)(3,5-DBQ)$_2$ is a classic valence tautomer studied extensively by conventional techniques such as EPR, UV−visible, Fourier transform infrared spectroscopy, and temperature-dependent magnetic susceptibility.[51,54] On the basis of prior studies[29] and magnetic susceptibility measurements in this and other work, the Co(phen) system interconverts between its

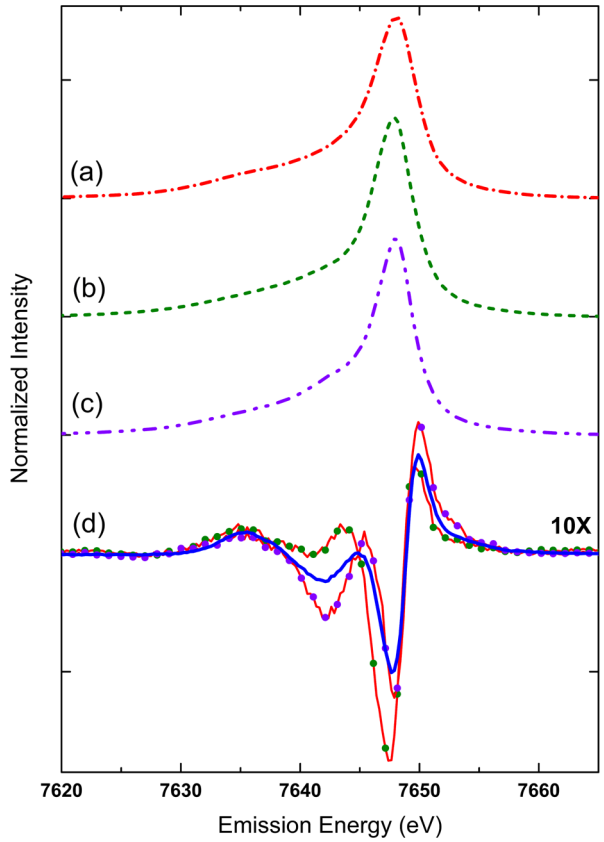

Figure 3. Co Kβ XES of (a) Co(phen)(3,5-DBQ)$_2$ taken at 34 K (red, dash-dotted line), (b) [Co(en)$_3$]Cl$_3$·2H$_2$O (dark green, dashed line), (c) Co(acac)$_3$ (purple, dash-dot-dotted line), where parts b and c are ls-Co^{III} reference model complexes, and (d) the difference spectra, defined as $I - I_{ref}$, of the low-*T* valence tautomer and ls-Co^{III} model complexes: Co(phen)(3,5-DBQ)$_2$ at 34 K with [Co(en)$_3$]Cl$_3$·2H$_2$O (red solid line + dark green solid circle) and Co(acac)$_3$ (red solid line + purple solid circle), along with a scaled (2×) difference spectrum generated from the hs-Co^{II} Co(acac)$_2$ and ls-Co^{III} Co(acac)$_3$ complexes (blue, solid line).

two valence tautomeric states at $T_{1/2} \approx 243$ K, whereas the Co(tmeda) system transitions at $T_{1/2} \approx 192$ K. The sharp increase in the magnetic moment of Co(tmeda) around $T_{1/2}$, as is evident in Figure 1c, signifies a narrow temperature range over which valence tautomerization occurs. By selecting a temperature far below their $T_{1/2}$ values, we ensure that both complexes are predominantly present in their low-*T* valence tautomeric state, Co(phen)(3,5-DBSQ)(3,5-DBCat) and Co(tmeda)(3,5-DBSQ)(3,5-DBCat), prior to X-ray exposure.

The Kβ XES spectra for Co(tmeda) at 36 K, [Co(en)$_3$]Cl$_3$·2H$_2$O and Co(acac)$_3$, and the differences between Co(tmeda) and these model complexes can be found in Figure 2. The strong similarity between the model spectra and valence tautomer with tmeda as its coligand demonstrates that low-*T* Co(tmeda) is well described by a single ls-Co^{III} $^1A_{1g}$ ($t_{2g}^6 e_g^0$) electronic configuration. Additionally, the shape of the difference spectra in Figure 2d does not support the presence of hs Co^{II} and thus rules out the observation of hard X-ray-induced valence tautomerization for Co(tmeda), as discussed in more detail in the Supporting Information, section I. The equivalence of the first and second XES spectra taken at the same sample position provides further support for the absence

DOI: 10.1021/acs.inorgchem.6b01666
Inorg. Chem. XXXX, XXX, XXX−XXX

of hard X-ray-induced valence tautomerization for Co(tmeda) (Figure S1).

Figure 3 shows the Kβ XES spectra for Co(phen) at 34 K, $[Co(en)_3]Cl_3 \cdot 2H_2O$ and $Co(acac)_3$, and the differences between Co(phen) and these model complexes along with a scaled difference plot generated from the hs-Co^{II} $Co(acac)_2$ and ls-Co^{III} $Co(acac)_3$ complexes. Unlike Co(tmeda), the low-*T* Co(phen) Kβ XES spectrum deviates significantly from the model complex spectra, with a deviation that strongly resembles the difference spectrum generated from $Co(acac)_2$ and $Co(acac)_3$. For this reason, we conclude that the low-*T* XES spectrum for Co(phen) shows the possibility of hard X-ray-induced VT, does not provide a clean measurement of the low-*T* valence tautomer, and cannot be used to determine the electronic structure of the low-*T* valence tautomeric state.

II. Assignment of the Oxidation and Spin States of Valence Tautomers at High Temperature Using Kβ XES. To establish the metal spin and oxidation states in the high-*T* valence tautomers, we collected Kβ XES spectra at 375 K, a temperature well above the $T_{1/2}$ value for both Co(phen) and Co(tmeda). Looking at Figure 4, the experimental Kβ XES spectra for the high-*T* valence tautomers resemble those of $Co(phen)_3 \cdot Cl_2 \cdot 4H_2O$ and $Co(acac)_2$, where the latter two complexes provide well-established models for hs Co^{II} with similar coordination geometry and bonding. In the hs-Co^{II} XES spectra, the K$\beta_{1,3}$ main peak has an asymmetric line shape with more spectral intensity at energies lower than the peak at 7649.0 eV. In addition, the presence of a broad Kβ' shoulder at 7636.0 eV provides the expected spectral signature associated with a hs-Co^{II} configuration, which is absent for a ls-Co^{II} XES (Figure S11).[60] The two hs-Co^{II} model complexes describe the spectral line shape of both high-*T* valence tautomers equally well, as is evident in their difference spectra in Figure 4e. Taken together, the high-*T* Co(phen) and Co(tmeda) valence tautomers are positively identified to be in a hs d^7 configuration, $t_{2g}^5e_g^2$, a conclusion supported by X-ray crystallography and other techniques.[51]

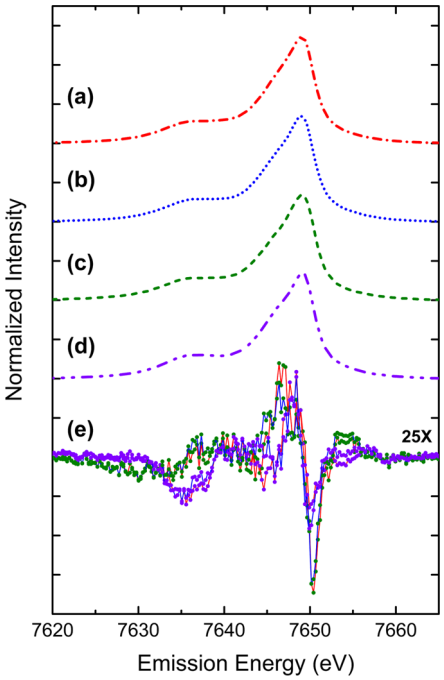

Figure 4. Co Kβ XES of (a) $Co(phen)(3,5\text{-}DBQ)_2$ taken at 375 K (red, dash-dotted line), (b) $Co(tmeda)(3,5\text{-}DBQ)_2$ taken at 375 K (blue, dotted line), (c) $Co(phen)_3 \cdot Cl_2 \cdot 4H_2O$ (dark green, dashed line), (d) $Co(acac)_2$ (purple, dash-dot-dotted line), where parts c and d are hs-Co^{II} reference model complexes, and (e) the difference spectra, defined as $I - I_{ref}$, of the high-*T* valence tautomers and hs-Co^{II} model complexes: $Co(phen)(3,5\text{-}DBQ)_2$ at 375 K with $Co(phen)_3 \cdot Cl_2 \cdot 4H_2O$ (red solid line + dark green solid circle) and $Co(acac)_2$ (red solid line + purple solid circle); $Co(tmeda)(3,5\text{-}DBQ)_2$ at 375 K with $Co(phen)_3 \cdot Cl_2 \cdot 4H_2O$ (blue solid line + dark green solid circle) and $Co(acac)_2$ (blue solid line + purple solid circle).

Results very similar to those observed in Co(phen) and Co(tmeda) have also been obtained for other cobalt valence tautomers in the high-*T* state, including Co(bpy), $Co(NO_2\text{-phen})$, Co(tmmda), and Co(tmpda), where bpy = 2,2′-bipyridine, NO_2-phen = 5-nitro-1,10-phenanthroline, tmmda = *N*,*N*,*N*′,*N*′-tetramethylmethylenediamine, and tmpda = *N*,*N*,*N*′,*N*′-tetramethylpropylenediamine (Figure S6). In all cases, the valence tautomers share the same spectral features and line shapes as the hs-Co^{II} model complexes, despite the varying σ-donor properties of their distinct nitrogen coligands. On the basis of the cobalt-specific XES data in this work, the σ-donor abilities of the nitrogen coligands do not tip the thermodynamic balance in favor of a ls-Co^{II} form at high temperature, as previously suggested by Adams et al.[61] The influence of the coligand on the transition temperature[51,54,62] does not lead to a change in the electron correlation at the Co center because the high-*T* valence tautomers all have the same hs-Co^{II} electronic configuration. Last, temperature-dependent Kβ XES measurements show two-state thermodynamics, as expected (see Figure S4).

III. Absence of hs-Co^{III} Electron Configurations in the High-*T* Valence Tautomeric State. Attempts to describe the electronic structure of cobalt valence tautomers have highlighted the potential importance of strong configuration interaction. In a combined theoretical and spectroscopic study by LaBute et al.,[39] they concluded that both hs-Co^{II} and hs-Co^{III} configurations contribute to the electronic structure of the high-*T* valence tautomers. To explore this possibility further, the Kβ XES spectra of $Co(phen)_3 \cdot Cl_2 \cdot 4H_2O$, one of the hs-$Co^{II}$ model complexes, and CoF_3, a rare example of a hs-Co^{III} octahedral species, are shown in Figure 5a. Compared to $Co(phen)_3 \cdot Cl_2 \cdot 4H_2O$, the positions of the K$\beta'$ shoulder for CoF_3 (7635.0 vs 7636.0 eV for the former) and the K$\beta_{1,3}$ main peak (7649.4 vs 7649.0 eV) are shifted to lower and higher emission energies, respectively, relative to the spectral center. Despite their dissimilar metal−ligand bonding interaction, the aforementioned spectral difference between CoF_3 and $Co(phen)_3 \cdot Cl_2 \cdot 4H_2O$ is confirmed by, and consistent with, our calculated hs-Co^{III} and hs-Co^{II} XES spectra (Figure S11). The spectral differences between Co(phen) at high-*T* and the two hs-Co model spectra appear in Figure 5b. On the basis of their variational configuration interaction analysis of the Co K preedge XAS, LaBute et al.[39] concluded that Co(phen) at high-*T* is comprised of 30% hs Co^{III} and 70% hs Co^{II}. The X-ray emission spectra of molecules with multiple configurations can be modeled as a weighted sum of single-electron configuration spectra, with amplitudes (α's) proportional to the contribution of each configuration to the overall electronic structure.[39,63,64] A multiconfigurational representation of the high-*T* valence tautomeric state is as follows:

$$|\psi_{\text{high-}T\ \text{VT}}\rangle = \alpha_1|\text{hs Co}^{\text{III}},\ d^6\rangle + \alpha_2|\text{hs Co}^{\text{II}},\ d^7\rangle$$

DOI: 10.1021/acs.inorgchem.6b01666
Inorg. Chem. XXXX, XXX, XXX−XXX

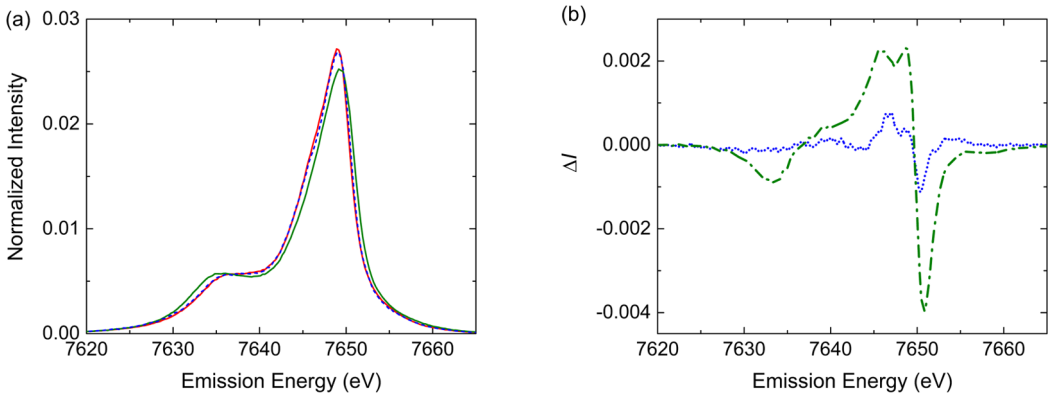

Figure 5. (a) Co Kβ XES of CoF_3 (dark green, solid line), a hs-Co^{III} reference model, $Co(phen)_3{\cdot}Cl_2{\cdot}4H_2O$ (blue, dashed line), a hs-Co^{II} reference model, and $Co(phen)(3,5\text{-}DBQ)_2$ taken at 375 K (red, solid line). (b) Difference spectra of $Co(phen)(3,5\text{-}DBSQ)_2$ with CoF_3 (dark green, dash-dotted line) and $Co(phen)_3{\cdot}Cl_2{\cdot}4H_2O$ (blue, dotted line). Note that ΔI is defined as $I - I_{ref}$.

where $|\psi_{\text{high-}T\ \text{VT}}\rangle$ is the complete wave function of the high-T valence tautomeric state and α_1 and α_2 are the coefficients for the corresponding electron configurations $|\text{hs Co}^{III}, d^6\rangle$ and $|\text{hs Co}^{II}, d^7\rangle$.

To test the significance of a hs-Co^{III} configuration, we fit the Co(phen) Kβ XES data to a linear sum of the $Co(phen)_3{\cdot}Cl_2{\cdot}4H_2O$ and CoF_3 spectra. Zero spectral weight for the hs-Co^{III} spectrum yields the minimum χ^2 fit and provides no evidence for a hs-Co^{III} configuration in the high-T valence tautomer.

IV. Co L-Edge XAS of the High-*T* Valence Tautomeric State. To further test if a hs-Co^{II} electron configuration alone best describes the metal center in valence tautomers, we used Co L-edge XAS to investigate both Co(phen) and Co(tmeda) at high temperature. Unlike Kβ XES, which probes the 3d valence electrons via its sensitivity to the 3p3d Coulomb and exchange interaction in the final states, Co L-edge XAS provides complementary information by examining the 3d unoccupied levels via optical excitation of a 2p core electron directly into 3d unfilled orbitals in an electric dipole-allowed transition.[65−69] Figure 6 shows the Co L-edge XAS of Co(phen) and Co(tmeda) at room temperature, as well as the hs-Co^{II} model complexes: $Co(phen)_3{\cdot}Cl_2{\cdot}4H_2O$ and $Co_4(3,5\text{-}DBSQ)_8$. The spectra of these complexes all show strong similarities. The additional intensity at 779.8 eV for Co(phen) can be explained by a small population of the low-T valence tautomers still present at 298.0 K, given its slightly higher $T_{1/2}$ value than that of Co(tmeda). The fast rate of soft X-ray-induced valence tautomerization precluded the use of Co L-edge XAS to characterize the valence tautomeric electronic structure at low-T.

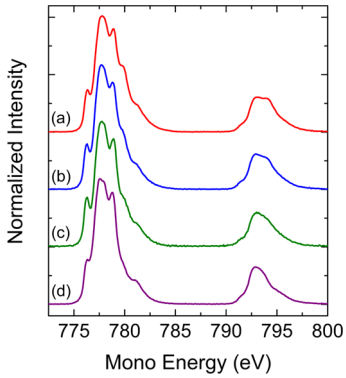

Figure 6. Co L-edge XAS of (a) $Co(phen)(3,5\text{-}DBSQ)_2$ (red, solid line), (b) $Co(tmeda)(3,5\text{-}DBSQ)_2$ (blue, solid line), (c) $Co(phen)_3{\cdot}Cl_2{\cdot}4H_2O$ (dark green, solid line), and (d) $Co_4(3,5\text{-}DBSQ)_8$ (purple, solid line). Both parts c and d are hs-Co^{II} reference model complexes. All of the spectra were taken at room temperature.

We also used ligand-field atomic-multiplet calculations to support the conclusions drawn from our X-ray measurements. The Co L-edge XAS of $Co_4(3,5\text{-}DBSQ)_8$ is compared side by side with the calculated hs-Co^{II} and hs-Co^{III} spectra (Figure 7).

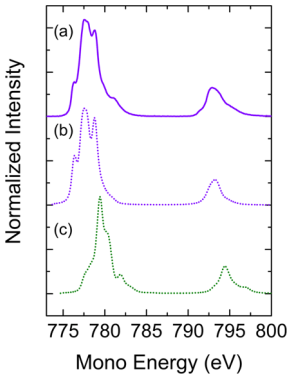

Figure 7. Comparison of Co L-edge XAS of (a) $Co_4(3,5\text{-}DBSQ)_8$ taken at room temperature (purple, solid line), a hs-Co^{II} reference compound, (b) calculated hs Co^{II} (purple, dotted line), and (c) calculated hs Co^{III} (dark green, dotted line). Note that the calculated spectra in parts b and c were scaled to the maximum peak height of the experimental data and red-shifted by 1.32 eV for comparison.

The calculations used an O_h molecular symmetry and a 10 Dq = 1.0 eV. The spectral shape for the calculated hs Co^{II} compares well with our L-edge spectra, but this is not the case with the calculated hs-Co^{III} spectrum. Note that the simulated Kβ XES spectra for hs Co^{II} and hs Co^{III} using the same atomic parameter settings compare well with their respective experimental data (Figure S11). Because an appropriate hs-Co^{III} model complex is lacking for the Co L-edge XAS measurements, we instead carried out extensive ligand-field atomic-multiplet calculations with different 10 Dq settings and Slater integral values (Figures S7−S9) to derive a comprehensive overview of the expected spectral shapes and features. These calculations further support the assignment of the high-T valence tautomer's electronic structure to a single determinant hs Co^{II}.

DOI: 10.1021/acs.inorgchem.6b01666
Inorg. Chem. XXXX, XXX, XXX−XXX

V. Magnetic Exchange Interaction between the Co Center and Semiquinonate Ligands in Valence Tautomers. Using Kβ XES, the spin state of the Co center in the two valence tautomeric states can be directly and unambiguously assigned. On the basis of the observation that the low-T state exists as a d^6, ls-Co^{III} center and the high-T state as a d^7, hs-Co^{II} center, there are nominally zero and three unpaired electrons found at the metal site, respectively. By relating the electronic information at the Co center determined using X-ray spectroscopies with the molecular magnetic moments of valence tautomers measured with SQUID magnetometry, new insight pertaining to the magnetic exchange interactions between the unpaired electrons on the metal center and those on the ligands can be deduced. The magnetic plots of Co(phen) and Co(tmeda) show simple two-state thermodynamics with weak intermolecular magnetic exchange interactions in the temperature range that we have studied with X-ray spectroscopy, unlike the strong temperature dependence of the magnetic properties that has been seen in similar $Co(SQ)_2$ valence tautomers at low temperature.[70,71] Taken together, the magnetic behaviors of our system allow for a straightforward interpretation in the temperature range of 25−375 K.

As observed in previous studies, the low-T valence tautomeric complexes have magnetic moments and EPR values consistent with those of one unpaired electron.[72,73] The Kβ emission spectra at low-T have been assigned to a ls-Co^{III} single electronic configuration, confirming that the unpaired electron is localized on a singly reduced semiquinone ligand.[61,72,74,75]

The Kβ emission spectra at high-T have been assigned to a hs-Co^{II} quartet electronic structure, with its three unpaired electrons distributed between the t_{2g} (dπ) and e_g (dσ) orbitals. It is coordinated to two semiquinonate ligands, each of which carries one unpaired electron in its valence orbital. Consequently, a total of five unpaired electrons are available to interact in the complex at high temperature. Consistent with previous magnetometry measurements,[51] the molecular spin moment is best assigned to $S = {}^3/_2$[76−80] and thus is inconsistent with the $S = {}^1/_2$ expected for strong antiferromagnetic coupling or the $S = {}^5/_2$ expected for strong ferromagnetic coupling between the hs quartet d^7 metal and doublet ligands. Given the absence of ls-Co^{II} configurations at high temperature, we can also rule out the possibility of a ferromagnetic molecular quartet with one unpaired electron on cobalt and each semiquinone.

In order to explain the metal−ligand magnetic exchange interaction based on a hs-Co^{II} center in valence tautomers at high-T, two alternate scenarios are possible. In the first and most probable scenario, the magnetic exchange interaction between cobalt and semiquinones is weak, on the order of a few millielectronvolts, such that the unpaired electrons on the ligands are weakly coupled to and oriented randomly with respect to the cobalt spin vector, an idea that was proposed by Pierpont and co-workers.[81−84] With a small-energy-level spacing between the $S = {}^1/_2, {}^3/_2, {}^5/_2$ electronic states, all spin configurations will be thermally populated at room temperature. Alternatively, the high-T state can be described as having a strong antiferromagnetic interaction between the spins on the semiquinone ligands. In this case, the two unpaired electrons on the ligands are presumed to pair opposite to each other, giving the ligands a total spin of $S = 0$ and yielding a coordination complex with a total spin of $S = {}^3/_2$. As a general conclusion from studies of $M(SQ)_3$ complexes, where the metal ion (M) is paramagnetic, M−SQ^- coupling is strong and antiferromagnetic for unpaired dπ metal electrons.[11,12,85] However, the hs d^7 center in our case, with only one unpaired spin in its dπ orbitals, does not support the case for strong M−L interactions.[86,87] Additionally, strong metal-mediated ligand−ligand interactions happen more often when the metal center is diamagnetic, not paramagnetic.[88,89] This reflects the shorter metal−ligand bond lengths in low-spin complexes, allowing for the proper orbital alignment to take place.[90] Again, that is not the case with the hs-Co^{II} center in the high-T valence tautomeric state; with its dσ orbitals half-filled, it is expected that a longer Co−O bond distance would result in weak Co−SQ^- bonding interactions, which matches with previous X-ray crystallography of the same valence tautomers studied at the two extreme temperatures.[51] Consequently, a scenario of strong antiferromagnetic interaction between two spatially separated SQ^-, mediated by a metal center with which they may only be weakly interacting, does not seem chemically or electronically likely. Nonetheless, this has been a popular theory among many groups.[20,88,91] Given our robust determination of the cobalt spin and oxidation states, in combination with experimental precedents on strong M−SQ^- interactions in $M(SQ)_3$ complexes and metal-mediated ligand−ligand interactions, we conclude that weak magnetic exchange interactions[92] between the Co and SQ^- ligands in the high-T valence tautomeric state provide the most probable description of the exchange interaction in these complexes.

■ CLOSING REMARKS

On the basis of the cobalt-specific, spin-sensitive Kβ XES and L-edge XAS, in conjunction with ligand-field atomic-multiplet calculations, it is evident that the Co center in both valence tautomeric states can be accurately modeled with single electronic configurations, ls Co^{III} in the low-T state and hs Co^{II} in the high-T state. We find no evidence for either ls-Co^{II} or hs-Co^{III} electronic configurations, as previously postulated to be of importance by Adams et al.[61] and LaBute et al.[39] This conclusion applies to numerous cobalt valence tautomers with chemically distinct N-donor coligands. For a limited number of nitrogen coligands, we observe that the coligand predominantly influences the transition temperatures, rather than the general electronic features, of the valence tautomers. In order to better understand the contribution and influence of nitrogen coligands in VT, further systematic investigations of different electron-withdrawing and -donating groups are needed.

By extending Kβ XES to the time domain, one can envision future studies dissecting the mechanism of photoinduced VT.[93−96] To convert the complex from the ls-Co^{III} state coordinated to a catecholate and a semiquinone ligand to the hs-Co^{II} state coordinated to two semiquinone ligands, one electron from the Cat^{2-} ligand has to be transferred to the metal via a ligand-to-metal charge-transfer excitation, thereby reducing the charge at the Co center and involving either a simultaneous or a sequential spin transition. While many research laboratories have attempted to address the thermally driven phenomenon via theoretical calculations,[39,40,61] this paper opens up the possibility of future photochemical studies—as previously demonstrated in various SCO systems[97−101]—on these transient spin and charge states of valence tautomers using Kβ XES in a time-resolved manner.

DOI: 10.1021/acs.inorgchem.6b01666
Inorg. Chem. XXXX, XXX, XXX−XXX

■ ASSOCIATED CONTENT

Supporting Information

The Supporting Information is available free of charge on the ACS Publications website at DOI: 10.1021/acs.inorgchem.6b01666.

Discussion of X-ray-induced VT, additional Kβ XES and difference emission spectra demonstrating the thermally driven valence tautomeric interconversion, and detailed ligand-field atomic-multiplet calculations of a hs-Co^{III} and a ls-Co^{II} center, along with concise descriptions of these spectral and calculated data (PDF)

■ AUTHOR INFORMATION

Corresponding Authors

*E-mail: wliang6@stanford.edu.
*E-mail: kgaffney@slac.stanford.edu.

ORCID

H. Winnie Liang: 0000-0001-6548-2061

Notes

The authors declare no competing financial interest.

■ ACKNOWLEDGMENTS

Use of the SSRL, SLAC National Accelerator Laboratory, is supported by the U.S. Department of Energy (DOE), Office of Science, Office of Basic Energy Sciences, under Contract DE-AC02-76SF00515. The SSRL Structural Molecular Biology Program is supported by the DOE, Office of Biological and Environmental Research, and by the National Institutes of Health, National Institute of General Medical Sciences (NIGMS; including Grant P41GM103393). The contents of this publication are solely the responsibility of the authors and do not necessarily represent the official views of the NIGMS or NIH. H.W.L. and K.J.G. acknowledge support from the AMOS program within the Chemical Sciences, Geosciences, and Biosciences Division of the Office of Basic Energy Sciences, Office of Science, DOE. H.W.L. acknowledges technical support from SSRL and sincerely thanks Dr. Shanina S. Johnson, Dr. Marco E. Reinhard, Dr. Trevor A. McQueen, and Hoang Nguyen for their assistance during the beamtimes as well as Dr. Maxwell C. Shapiro and Professor Ian Fisher for the use of their MPMS instrument and helpful discussions.

■ REFERENCES

(1) Sato, O.; Tao, J.; Zhang, Y. Control of Magnetic Properties through External Stimuli. *Angew. Chem., Int. Ed.* **2007**, *46*, 2152−2187.

(2) Boskovic, C. Valence Tautomeric Transitions in Cobalt-Dioxolene Complexes. In *Spin-Crossover Materials: Properties and Applications*; Halcrow, M. A., Ed.; John Wiley & Sons Ltd.: New York, 2013; pp 203−224.

(3) *Spin-Crossover Materials: Properties and Applications*; Halcrow, M. A., Ed.; John Wiley & Sons, Ltd.: Chichester, U.K., 2013.

(4) Calzolari, A.; Chen, Y.; Lewis, G. F.; Dougherty, D. B.; Shultz, D.; Nardelli, M. B. Complex Materials for Molecular Spintronics Applications: Cobalt Bis(dioxolene) Valence Tautomers, from Molecules to Polymers. *J. Phys. Chem. B* **2012**, *116*, 13141−13148.

(5) Novio, F.; Campo, J.; Ruiz-Molina, D. Controlling Spin Transition in One-Dimensional Coordination Polymers through Polymorphism. *Inorg. Chem.* **2014**, *53*, 8742−8748.

(6) Sato, O. Dynamic Molecular Crystals with Switchable Physical Properties. *Nat. Chem.* **2016**, *8*, 644−656.

(7) Li, W.; Geng, Z.; Wang, Y.; Zhang, X.; Wang, Z.; Liu, F. DFT Studies of Thermal Activation of Methane by $[Ru(H)(OH)]^+$. *J. Mol. Struct.: THEOCHEM* **2009**, *897*, 86−89.

(8) Schweitzer, D.; Shearer, J.; Rittenberg, D. K.; Shoner, S. C.; Ellison, J. J.; Loloee, R.; Lovell, S.; Barnhart, D.; Kovacs, J. A. Enhancing Reactivity via Structural Distortion. *Inorg. Chem.* **2002**, *41*, 3128−3136.

(9) Minaev, B.; Baryshnikova, A.; Sun, W. Spin-Dependent Effects in Ethylene Polymerization with Bis(imino) Pyridine Iron(II) Complexes. *J. Organomet. Chem.* **2016**, *811*, 48−65.

(10) Pierpont, C. G. Studies on Charge Distribution and Valence Tautomerism in Transition Metal Complexes of Catecholate and Semiquinonate Ligands. *Coord. Chem. Rev.* **2001**, *216−217*, 99−125.

(11) Pierpont, C. G.; Lange, C. W., The Chemistry of Transition Metal Complexes Containing Catechol and Semiquinone Ligands. *Progress in Inorganic Chemistry*; John Wiley & Sons, Inc.: New York, 2007; pp 331−442.

(12) Hendrickson, D. N.; Pierpont, C. G. Valence Tautomeric Transition Metal Complexes. *Spin Crossover in Transition Metal Compounds II*; Springer: Berlin, 2004; Vol. *234*, pp 63−95.

(13) Pierpont, C. G.; Buchanan, R. M. Transition Metal Complexes of *o*-Benzoquinone, *o*-Semiquinone, and Catecholate Ligands. *Coord. Chem. Rev.* **1981**, *38*, 45−87.

(14) Evangelio, E.; Ruiz-Molina, D. Valence Tautomerism: New Challenges for Electroactive Ligands. *Eur. J. Inorg. Chem.* **2005**, *2005*, 2957−2971.

(15) Tezgerevska, T.; Alley, K. G.; Boskovic, C. Valence Tautomerism in Metal Complexes: Stimulated and Reversible Intramolecular Electron Transfer between Metal Centers and Organic Ligands. *Coord. Chem. Rev.* **2014**, *268*, 23−40.

(16) Dei, A.; Gatteschi, D.; Sangregorio, C.; Sorace, L. Quinonoid Metal Complexes: Toward Molecular Switches. *Acc. Chem. Res.* **2004**, *37*, 827−835.

(17) Gaspar, A. B.; Seredyuk, M. Spin Crossover in Soft Matter. *Coord. Chem. Rev.* **2014**, *268*, 41−58.

(18) Vazquez-Mera, N. A.; Roscini, C.; Hernando, J.; Ruiz-Molina, D. Liquid-Filled Valence Tautomeric Microcapsules: A Solid Material with Solution-Like Behavior. *Adv. Funct. Mater.* **2015**, *25*, 4129−4134.

(19) Sato, O. Switchable Molecular Magnets. *Proc. Jpn. Acad., Ser. B* **2012**, *88*, 213−225.

(20) Protasenko, N. A.; Poddel'sky, A. I.; Bogomyakov, A. S.; Somov, N. V.; Abakumov, G. A.; Cherkasov, V. K. Bis-*o*-Semiquinonato Complexes of Transition Metals with 5,7-Di-Tert-Butyl-2-(Pyridine-2-yl)Benzoxazole. *Polyhedron* **2013**, *49*, 239−243.

(21) Weiss, R.; Bulach, V.; Gold, A.; Terner, J.; Trautwein, A. Valence-Tautomerism in High-Valent Iron and Manganese Porphyrins. *JBIC, J. Biol. Inorg. Chem.* **2001**, *6*, 831−845.

(22) Attia, A. S.; Pierpont, C. G. Valence Tautomerism for Quinone Complexes of Manganese: Members of the Mn^{IV}(N-N) $(Cat)_2$-Mn^{III}(N-N) (SQ) (Cat)-Mn^{II}(N-N) $(SQ)_2$ Series. *Inorg. Chem.* **1995**, *34*, 1172−1179.

(23) Evangelio, E.; Ruiz-Molina, D. Valence Tautomerism: More Actors Than Just Electroactive Ligands and Metal Ions. *C. R. Chim.* **2008**, *11*, 1137−1154.

(24) Gütlich, P.; Dei, A. Valence Tautomeric Interconversion in Transition Metal 1,2-Benzoquinone Complexes. *Angew. Chem., Int. Ed. Engl.* **1997**, *36*, 2734−2736.

(25) Rotthaus, O.; Thomas, F.; Jarjayes, O.; Philouze, C.; Saint-Aman, E.; Pierre, J.-L. Valence Tautomerism in Octahedral and Square-Planar Phenoxyl-Nickel(II) Complexes: Are Imino Nitrogen Atoms Good Friends? *Chem. - Eur. J.* **2006**, *12*, 6953−6962.

(26) Kanegawa, S.; Kang, S.; Sato, O. Preparation and Valence Tautomeric Behavior of a Cobalt-Dioxolene Complex with a New TTF-functionalized Phenanthroline Ligand. *Chem. Lett.* **2013**, *42*, 700−702.

(27) Ando, I.; Fukuishi, T.; Ujimoto, K.; Kurihara, H. Oxidation States and Redox Behavior of Ruthenium Ammine Complexes with Redox-Active Dioxolene Ligands. *Inorg. Chim. Acta* **2012**, *390*, 47−52.

(28) Witt, A.; Heinemann, F. W.; Khusniyarov, M. M. Bidirectional Photoswitching of Magnetic Properties at Room Temperature: Ligand-Driven Light-Induced Valence Tautomerism. *Chem. Sci.* **2015**, *6*, 4599−4609.

DOI: 10.1021/acs.inorgchem.6b01666
Inorg. Chem. XXXX, XXX, XXX−XXX

(29) Sato, O.; Hayami, S.; Gu, Z. Z.; Takahashi, K.; Nakajima, R.; Seki, K.; Fujishima, A. Photo-Induced Valence Tautomerism in a Co Compound. *J. Photochem. Photobiol., A* **2002**, *149*, 111−114.
(30) Adams, D. M.; Li, B. L.; Simon, J. D.; Hendrickson, D. N. Photoinduced Valence Tautomerism in Cobalt Bis-o-Quinone Complexes: Dynamics of High-Spin $Co^{II}(3,5\text{-DTBSQ})_2$ to Low-Spin Co^{III}(3,5-DTBCAT) Interconversion. *Angew. Chem., Int. Ed. Engl.* **1995**, *34*, 1481.
(31) Roux, C.; Adams, D. M.; Itié, J. P.; Polian, A.; Hendrickson, D. N.; Verdaguer, M. Pressure-Induced Valence Tautomerism in Cobalt o-Quinone Complexes: An X-ray Absorption Study of the Low-Spin [Co^{III}(3,5-DTBSQ)(3,5-DTBCat) (phen)] to High-Spin [$Co^{II}(3,5\text{-DTBSQ})_2$(phen)] Interconversion. *Inorg. Chem.* **1996**, *35*, 2846−2852.
(32) Poneti, G.; Mannini, M.; Sorace, L.; Sainctavit, P.; Arrio, M.-A.; Otero, E.; Criginski Cezar, J.; Dei, A. Soft-X-ray-Induced Redox Isomerism in a Cobalt Dioxolene Complex. *Angew. Chem., Int. Ed.* **2010**, *49*, 1954−1957.
(33) Tao, J.; Maruyama, H.; Sato, O. Valence Tautomeric Transitions with Thermal Hysteresis around Room Temperature and Photo-induced Effects Observed in a Cobalt−Tetraoxolene Complex. *J. Am. Chem. Soc.* **2006**, *128*, 1790−1791.
(34) Slota, M.; Blankenhorn, M.; Heintze, E.; Vu, M.; Huebner, R.; Bogani, L. Photoswitchable Stable Charge-Distributed States in a New Cobalt Complex Exhibiting Photo-Induced Valence Tautomerism. *Faraday Discuss.* **2015**, *185*, 347−359.
(35) Caneschi, A.; Dei, A.; Fabrizi de Biani, F.; Gutlich, P.; Ksenofontov, V.; Levchenko, G.; Hoefer, A.; Renz, F. Pressure- and Temperature-Induced Valence Tautomeric Interconversion in a *o*-Dioxolene Adduct of a Cobalt-Tetraazamacrocycle Complex. *Chem. - Eur. J.* **2001**, *7*, 3926−3930.
(36) Poneti, G.; Mannini, M.; Sorace, L.; Sainctavit, P.; Arrio, M.-A.; Rogalev, A.; Wilhelm, F.; Dei, A. X-ray Absorption Spectroscopy as a Probe of Photo- and Thermally Induced Valence Tautomeric Transition in a 1:1 Cobalt−Dioxolene Complex. *ChemPhysChem* **2009**, *10*, 2090−2095.
(37) Yokoyama, T.; Okamoto, K.; Nagai, K.; Ohta, T.; Hayami, S.; Gu, Z. Z.; Nakajima, R.; Sato, O. Photo-induced magnetized state of Co(DTBSQ) (DTBCat) (phen) center dot $C_6H_5CH_3$ studied by X-ray absorption spectroscopy. *Chem. Phys. Lett.* **2001**, *345*, 272−276.
(38) LaBute, M.; Kulkarni, R.; Endres, R.; Cox, D. Strong Electron Correlations in Cobalt Valence Tautomers: Evidence from X-ray Absorption. *APS Meeting Abstracts*; American Physical Society: Indiana, 2002; p 30007.
(39) LaBute, M. X.; Kulkarni, R. V.; Endres, R. G.; Cox, D. L. Strong Electron Correlations in Cobalt Valence Tautomers. *J. Chem. Phys.* **2002**, *116*, 3681−3689.
(40) Sato, D.; Shiota, Y.; Juhász, G.; Yoshizawa, K. Theoretical Study of the Mechanism of Valence Tautomerism in Cobalt Complexes. *J. Phys. Chem. A* **2010**, *114*, 12928−12935.
(41) Pollock, C. J.; Delgado-Jaime, M. U.; Atanasov, M.; Neese, F.; DeBeer, S. K_β Mainline X-ray Emission Spectroscopy as an Experimental Probe of Metal−Ligand Covalency. *J. Am. Chem. Soc.* **2014**, *136*, 9453−9463.
(42) Pollock, C. J.; DeBeer, S. Valence-to-Core X-ray Emission Spectroscopy: A Sensitive Probe of the Nature of a Bound Ligand. *J. Am. Chem. Soc.* **2011**, *133*, 5594−5601.
(43) Lancaster, K. M.; Finkelstein, K. D.; DeBeer, S. K_β X-ray Emission Spectroscopy Offers Unique Chemical Bonding Insights: Revisiting the Electronic Structure of Ferrocene. *Inorg. Chem.* **2011**, *50*, 6767−6774.
(44) De Groot, F.; Kotani, A. *Core Level Spectroscopy of Solids*; CRC Press, Taylor & Francis Group: Boca Raton, FL, 2008; p 512.
(45) Escax, V.; Bleuzen, A.; Itié, J. P.; Munsch, P.; Varret, F.; Verdaguer, M. Nature of the Long-Range Structural Changes Induced by the Molecular Photoexcitation and by the Relaxation in the Prussian Blue Analogue $Rb_{1.8}Co_4[Fe(CN)_6]_{3.3}\cdot 13H_2O$. A Synchrotron X-ray Diffraction Study. *J. Phys. Chem. B* **2003**, *107*, 4763−4767.
(46) Vankó, G.; Renz, F.; Molnár, G.; Neisius, T.; Kárpáti, S. Hard-X-ray-Induced Excited-Spin-State Trapping. *Angew. Chem., Int. Ed.* **2007**, *46*, 5306−5309.
(47) Kiryukhin, V.; Casa, D.; Hill, J. P.; Keimer, B.; Vigliante, A.; Tomioka, Y.; Tokura, Y. An X-ray-Induced Insulator-Metal Transition in a Magnetoresistive Manganite. *Nature* **1997**, *386*, 813−815.
(48) Bleuzen, A.; Marvaud, V.; Mathoniere, C.; Sieklucka, B.; Verdaguer, M. Photomagnetism in Clusters and Extended Molecule-Based Magnets. *Inorg. Chem.* **2009**, *48*, 3453−3466.
(49) Margadonna, S.; Prassides, K.; Fitch, A. N. Large Lattice Responses in a Mixed-Valence Prussian Blue Analogue Owing to Electronic and Spin Transitions Induced by X-ray Irradiation. *Angew. Chem., Int. Ed.* **2004**, *43*, 6316−6319.
(50) Papanikolaou, D.; Margadonna, S.; Kosaka, W.; Ohkoshi, S.-i.; Brunelli, M.; Prassides, K. X-ray Illumination Induced Fe(II) Spin Crossover in the Prussian Blue Analogue Cesium Iron Hexacyanochromate. *J. Am. Chem. Soc.* **2006**, *128*, 8358−8363.
(51) Adams, D. M.; Dei, A.; Rheingold, A. L.; Hendrickson, D. N. Bistability in the [$Co^{II}(\text{Semiquinonate})_2$] to [$Co^{III}$(Catecholate) (Semiquinonate)] Valence-Tautomeric Conversion. *J. Am. Chem. Soc.* **1993**, *115*, 8221−8229.
(52) Yamasaki, K.; Hara, T.; Yasuda, M. Absorption Spectra of Cobalt Complexes with 1, 10-Phenanthroline. *Proc. Jpn. Acad.* **1953**, *29*, 337−341.
(53) Liu, W.; Xu, W.; Lin, J.; Xie, H. Tris(2,2′-Bipyridine-κ^2 N:N′)Cobalt(III) Trichloride Tetrahydrate. *Acta Crystallogr., Sect. E: Struct. Rep. Online* **2008**, *64*, m1586−m1586.
(54) Jung, O.-S.; Pierpont, C. G. Bistability and Low-Energy Electron Transfer in Cobalt Complexes Containing Catecholate and Semiquinone Ligands. *Inorg. Chem.* **1994**, *33*, 2227−2235.
(55) Stavitski, E.; de Groot, F. M. F. The CTM4XAS Program for EELS and XAS Spectral Shape Analysis of Transition Metal *L*-Edges. *Micron* **2010**, *41*, 687−694.
(56) de Groot, F. M. F.; Fuggle, J. C.; Thole, B. T.; Sawatzky, G. A. 2*p* X-ray Absorption of 3*d* Transition-Metal Compounds: An Atomic Multiplet Description Including the Crystal Field. *Phys. Rev. B: Condens. Matter Mater. Phys.* **1990**, *42*, 5459.
(57) Suenaga, Y.; Pierpont, C. G. Binuclear Complexes of Co(III) Containing Extended Conjugated Bis(Catecholate) Ligands. *Inorg. Chem.* **2005**, *44*, 6183−6191.
(58) Jung, O.-S.; Jo, D. H.; Lee, Y.-A.; Conklin, B. J.; Pierpont, C. G. Bistability and Molecular Switching for Semiquinone and Catechol Complexes of Cobalt. Studies on Redox Isomerism for the Bis(pyridine) Ether Series $Co(py_2X)(3,6\text{-DBQ})_2$, X = O, S, Se, and Te. *Inorg. Chem.* **1997**, *36*, 19−24.
(59) Tourón Touceda, P.; Mosquera Vazquez, V. S.; Lima, M.; Lapini, A.; Foggi, P.; Dei, A.; Righini, R. Transient Infrared Spectroscopy: a New Approach to Investigate Valence Tautomerism. *Phys. Chem. Chem. Phys.* **2012**, *14*, 1038−1047.
(60) Vankó, G.; Neisius, T.; Molnár, G.; Renz, F.; Kárpáti, S.; Shukla, A.; de Groot, F. M. F. Probing the 3*d* Spin Momentum with X-ray Emission Spectroscopy: The Case of Molecular-Spin Transitions. *J. Phys. Chem. B* **2006**, *110*, 11647−11653.
(61) Adams, D. M.; Noodleman, L.; Hendrickson, D. N. Density Functional Study of the Valence-Tautomeric Interconversion Low-Spin [Co^{III}(SQ) (Cat) (phen)] ⇌ High-Spin [$Co^{II}(SQ)_2$(phen)]. *Inorg. Chem.* **1997**, *36*, 3966−3984.
(62) Jung, O.-S.; Jo, D. H.; Lee, Y.-A.; Sohn, Y. S.; Pierpont, C. G. Chelate-Ring-Dependent Shifts in Redox Isomerism for the Co-$(Me_2N(CH_2)_nNMe_2)(3,6\text{-DBQ})_2$ (n = 1−3) Series, Where 3,6-DBQ Is the Semiquinonate or Catecholate Ligand Derived from 3,6-Di-tert-butyl-1,2-benzoquinone. *Inorg. Chem.* **1998**, *37*, 5875−5880.
(63) Dolg, M. *Computational Methods in Lanthanide and Actinide Chemistry*; Wiley: New York, 2015.
(64) Booth, C. H.; Kazhdan, D.; Werkema, E. L.; Walter, M. D.; Lukens, W. W.; Bauer, E. D.; Hu, Y.-J.; Maron, L.; Eisenstein, O.; Head-Gordon, M.; Andersen, R. A. Intermediate-Valence Tautomerism in Decamethylytterbocene Complexes of Methyl-Substituted Bipyridines. *J. Am. Chem. Soc.* **2010**, *132*, 17537−17549.

DOI: 10.1021/acs.inorgchem.6b01666
Inorg. Chem. XXXX, XXX, XXX−XXX

(65) Wilson, S. A.; Kroll, T.; Decreau, R. A.; Hocking, R. K.; Lundberg, M.; Hedman, B.; Hodgson, K. O.; Solomon, E. I. Iron *L*-Edge X-ray Absorption Spectroscopy of Oxy-Picket Fence Porphyrin: Experimental Insight into Fe−O_2 Bonding. *J. Am. Chem. Soc.* **2013**, *135*, 1124−1136.

(66) Hocking, R. K.; Wasinger, E. C.; Yan, Y.-L.; deGroot, F. M. F.; Walker, F. A.; Hodgson, K. O.; Hedman, B.; Solomon, E. I. Fe *L*-Edge X-ray Absorption Spectroscopy of Low-Spin Heme Relative to Non-heme Fe Complexes: Delocalization of Fe *d*-Electrons into the Porphyrin Ligand. *J. Am. Chem. Soc.* **2007**, *129*, 113−125.

(67) Wang, H.; Peng, G.; Miller, L. M.; Scheuring, E. M.; George, S. J.; Chance, M. R.; Cramer, S. P. Iron *L*-Edge X-ray Absorption Spectroscopy of Myoglobin Complexes and Photolysis Products. *J. Am. Chem. Soc.* **1997**, *119*, 4921−4928.

(68) Cramer, S. P.; DeGroot, F. M. F.; Ma, Y.; Chen, C. T.; Sette, F.; Kipke, C. A.; Eichhorn, D. M.; Chan, M. K.; Armstrong, W. H. Ligand Field Strengths and Oxidation States from Manganese *L*-Edge Spectroscopy. *J. Am. Chem. Soc.* **1991**, *113*, 7937−7940.

(69) Jayarathne, U.; Chandrasekaran, P.; Greene, A. F.; Mague, J. T.; DeBeer, S.; Lancaster, K. M.; Sproules, S.; Donahue, J. P. X-ray Absorption Spectroscopy Systematics at the Tungsten *L*-Edge. *Inorg. Chem.* **2014**, *53*, 8230−8241.

(70) Bencini, A.; Beni, A.; Costantino, F.; Dei, A.; Gatteschi, D.; Sorace, L. The influence of Ligand Field Effects on the Magnetic Exchange of High-Spin Co(II)-Semiquinonate Complexes. *Dalton Trans.* **2006**, 722−729.

(71) Beni, A.; Dei, A.; Laschi, S.; Rizzitano, M.; Sorace, L. Tuning the Charge Distribution and Photoswitchable Properties of Cobalt−Dioxolene Complexes by Using Molecular Techniques. *Chem. - Eur. J.* **2008**, *14*, 1804−1813.

(72) Buchanan, R. M.; Pierpont, C. G. Tautomeric Catecholate-Semiquinone Interconversion via Metal-Ligand Electron Transfer. Structural, Spectral, and Magnetic Properties of (3,5-Di-Tert-Butylcatecholato)(3,5-Di-Tert-Butylsemiquinone) (Bipyridyl)Cobalt-(III), a Complex Containing Mixed-Valence Organic Ligands. *J. Am. Chem. Soc.* **1980**, *102*, 4951−4957.

(73) Larsen, S. K.; Pierpont, C. G. Cobalt and Manganese Complexes of a Schiff Base Biquinone Radical Ligand. *J. Am. Chem. Soc.* **1988**, *110*, 1827−1832.

(74) Abakumov, G. A.; Bubnov, M. P.; Éllert, O. G.; Dobrokhotova, Zh. B.; Zakharov, L. N.; Struchkov, Yu. T. Redox Isomerism of Paramagnetic Cobalt o-Semiquinone Complexes in the Solid Phase. Study of Co(bpy) $(SQ)_2$ Compounds by X-ray Diffraction Structural Analysis, Magnetochemistry, ESR Spectroscopy, and Scanning Calorimetry. *Dokl. Akad. Nauk* **1993**, *328*, 332−335.

(75) Kadohashi, Y.; Maruta, G.; Takeda, S. Spin and Charge Fluctuation Occurring in Valence Tautomerism and Cooperative Effects in the Solid-State. *Polyhedron* **2007**, *26*, 2342−2346.

(76) Figgis, B. N.; Nyholm, R. S. 61. Magnetochemistry. Part II. The Temperature-Dependence of the Magnetic Susceptibility of Bivalent Cobalt Compounds. *J. Chem. Soc.* **1959**, 338−345.

(77) Stoufer, R. C.; Busch, D. H.; Hadley, W. B. Unusual Magnetic Properties of Some Six-Coordinate Cobalt(II) Complexes — Electronic Isomers. *J. Am. Chem. Soc.* **1961**, *83*, 3732−3734.

(78) Figgis, B. N.; Nyholm, R. S. Magnetic Moments and Stereochemistry of Cobaltous Compounds. *J. Chem. Soc.* **1954**, 12−15.

(79) Burstall, F. H.; Nyholm, R. S. 681. Studies in Coordination Chemistry. Part XIII. Magnetic Moments and Bond Types of Transition-Metal Complexes. *J. Chem. Soc.* **1952**, 3570−3579.

(80) Jha, N. N.; Ray, I. P. Magnetic Studies on Co(II) and Ni(II) Complexes of Hydroxamic Acid. *Asian J. Chem.* **2000**, *12*, 703−706.

(81) Lynch, M. W.; Buchanan, R. M.; Pierpont, C. G.; Hendrickson, D. N. Weak Magnetic Exchange Interactions between Paramagnetic Metal Ions and Coordinated *o*-Semiquinones in M(9,10-Phenanthrenesemiquinone)$_2$(Pyridine)$_2$ [M = Nickel(II) and Cobalt(II)] and Tetranuclear M_4(*o*-Semiquinone)$_8$ Complexes. *Inorg. Chem.* **1981**, *20*, 1038−1046.

(82) Pavlova, N. A.; Poddel'sky, A. I.; Bogomyakov, A. S.; Fukin, G. K.; Cherkasov, V. K.; Abakumov, G. A. New High-Spin Bis-*o*-Semiquinonato Cobalt(II) Complexes with Neutral Donor Ligands. *Inorg. Chem. Commun.* **2011**, *14*, 1661−1664.

(83) Klokishner, S. I.; Reu, O. S. Vibronic Dynamic Problem of Valence Tautomerism in Cobalt Compounds. Magnetic and Optical Properties. *Polyhedron* **2003**, *22*, 2401−2408.

(84) Pierpont, C. G.; Kelly, J. K. Coordination Chemistry of *o*-Semiquinones. *PATAI'S Chemistry of Functional Groups*; John Wiley & Sons, Ltd.: New York, 2009.

(85) Buchanan, R. M.; Kessel, S. L.; Downs, H. H.; Pierpont, C. G.; Hendrickson, D. N. Structural and Magnetic Properties of Tris(*o*-Semiquinone) Complexes of Iron(III) and Chromium(III). *J. Am. Chem. Soc.* **1978**, *100*, 7894−7900.

(86) Sik Min, K.; Weyhermuller, T.; Wieghardt, K. Coordination Chemistry of 2-(8-Aminoquinolino)-4,6-Di-Tert-Butylphenol with Manganese(IV), Iron(III), and Cobalt(II/III): N,O-Coordinated *o*-Iminobenzosemiquinonate(1-) pi Radical Monoanions vs. *o*-Iminophenolate(2-) dianions. *Dalton Trans.* **2004**, 178−186.

(87) Klokishner, S. Cobalt Valence Tautomeric Compounds: Molecular and Solid State Properties. *Chem. Phys.* **2001**, *269*, 411−440.

(88) Caneschi, A.; Dei, A.; Gatteschi, D.; Tangoulis, V. Antiferromagnetic Coupling in a Six-Coordinate High Spin Cobalt-(II)−Semiquinonato Complex. *Inorg. Chem.* **2002**, *41*, 3508−3512.

(89) Lange, C. W.; Conklin, B. J.; Pierpont, C. G. Radical Superexchange in Semiquinone Complexes Containing Diamagnetic Metal-Ions - 3,6-Di-Tert-Butyl-1,2-Semiquinonate Complexes of Zinc(II), Cobalt(III), Gallium(III), and Aluminum(III). *Inorg. Chem.* **1994**, *33*, 1276−1283.

(90) Bruni, S.; Caneschi, A.; Cariati, F.; Delfs, C.; Dei, A.; Gatteschi, D. Ferromagnetic Coupling between Semiquinone Type Tridentate Radical Ligands Mediated by Metal-Ions. *J. Am. Chem. Soc.* **1994**, *116*, 1388−1394.

(91) Zolotukhin, A. A.; Bubnov, M. P.; Bogomyakov, A. S.; Protasenko, N. A.; Fukin, G. K.; Grishin, I. D.; Cherkasov, V. K. Binuclear Bis(o-Semiquinonato)Cobalt(II) Complexes with Bridging Tetradentate N-Donor Ligand. *Inorg. Chim. Acta* **2016**, *440*, 16−20.

(92) Witt, A.; Heinemann, F. W.; Sproules, S.; Khusniyarov, M. M. Modulation of Magnetic Properties at Room Temperature: Coordination-Induced Valence Tautomerism in a Cobalt Dioxolene Complex. *Chem. - Eur. J.* **2014**, *20*, 11149−11162.

(93) Gentili, P. L.; Bussotti, L.; Righini, R.; Beni, A.; Bogani, L.; Dei, A. Time-Resolved Spectroscopic Characterization of Photo-Induced Valence Tautomerism for a Cobalt-Dioxolene Complex. *Chem. Phys.* **2005**, *314*, 9−17.

(94) Cui, A.; Takahashi, K.; Fujishima, A.; Sato, O. Mechanism and Relaxation Kinetics of Photo-Induced Valence Tautomerism of Co(Phen)(3,5-DBSQ)$_2$*C_6H_5Cl. *J. Photochem. Photobiol., A* **2004**, *167*, 69−73.

(95) Beni, A.; Bogani, L.; Bussotti, L.; Dei, A.; Gentili, P. L.; Righini, R. Characterization of Photo-Induced Valence Tautomerism in a Cobalt-Dioxolene Complex by Ultrafast Spectroscopy. In *Second International Conference on Photo-Induced Phase Transitions: Cooperative, Nonlinear and Functional Properties*, Buron, M., Collet, E., Eds.; Journal of Physics: Conference Series, Rennes, France, 2005; Vol. *21*, pp 124−129.

(96) Adams, D. M.; Hendrickson, D. N. Pulsed Laser Photolysis and Thermodynamics Studies of Intramolecular Electron Transfer in Valence Tautomeric Cobalt *o*-Quinone Complexes. *J. Am. Chem. Soc.* **1996**, *118*, 11515−11528.

(97) Vankó, G.; Bordage, A.; Glatzel, P.; Gallo, E.; Rovezzi, M.; Gawelda, W.; Galler, A.; Bressler, C.; Doumy, G.; March, A. M.; Kanter, E. P.; Young, L.; Southworth, S. H.; Canton, S. E.; Uhlig, J.; Smolentsev, G.; Sundström, V.; Haldrup, K.; van Driel, T. B.; Nielsen, M. M.; Kjaer, K. S.; Lemke, H. T. Spin-State Studies with XES and RIXS: From Static to Ultrafast. *J. Electron Spectrosc. Relat. Phenom.* **2013**, *188*, 166−171.

(98) Chergui, M. Time-Resolved X-ray Spectroscopies of Chemical Systems: New Perspectives. *Struct. Dyn.* **2016**, *3*, 031001.

DOI: 10.1021/acs.inorgchem.6b01666
Inorg. Chem. XXXX, XXX, XXX−XXX

(99) Zhang, W.; Alonso-Mori, R.; Bergmann, U.; Bressler, C.; Chollet, M.; Galler, A.; Gawelda, W.; Hadt, R. G.; Hartsock, R. W.; Kroll, T.; Kjaer, K. S.; Kubicek, K.; Lemke, H. T.; Liang, H. W.; Meyer, D. A.; Nielsen, M. M.; Purser, C.; Robinson, J. S.; Solomon, E. I.; Sun, Z.; Sokaras, D.; van Driel, T. B.; Vanko, G.; Weng, T.-C.; Zhu, D.; Gaffney, K. J. Tracking Excited-State Charge and Spin Dynamics in Iron Coordination Complexes. *Nature* **2014**, *509*, 345−348.

(100) Vankó, G.; Glatzel, P.; Pham, V.-T.; Abela, R.; Grolimund, D.; Borca, C. N.; Johnson, S. L.; Milne, C. J.; Bressler, C. Picosecond Time-Resolved X-Ray Emission Spectroscopy: Ultrafast Spin-State Determination in an Iron Complex. *Angew. Chem., Int. Ed.* **2010**, *49*, 5910−5912.

(101) Bressler, C.; Gawelda, W.; Galler, A.; Nielsen, M. M.; Sundstrom, V.; Doumy, G.; March, A. M.; Southworth, S. H.; Young, L.; Vanko, G. Solvation Dynamics Monitored by Combined X-ray Spectroscopies and Scattering: Photoinduced Spin Transition in Aqueous $[Fe(bpy)_3]^{2+}$. *Faraday Discuss.* **2014**, *171*, 169−178.

DOI: 10.1021/acs.inorgchem.6b01666
Inorg. Chem. XXXX, XXX, XXX−XXX